

Supporting Information

3D-(p/p/n) NiO/NiWO₄/WO₃ Heterostructures for Selective Detection of Ozone

Navpreet Kaur,^{a*} and Elisabetta Comini^a

^a SENSOR Laboratory, Department of Information Engineering (DII), University of Brescia, Via D. Valotti 9, Brescia 25133, Italy

Email: navpreet.kaur@unibs.it

Response and recovery time

The response and recovery time of the sensor was calculated when the response reached 90 % and recovery at 70 %. Indeed, both these values are overestimated because of the limitations of the test chamber which required 5-10 minutes to fill the full volume (1L) of the stainless-steel chamber. Thus, in real, much lesser values can be expected for both response and recovery times.

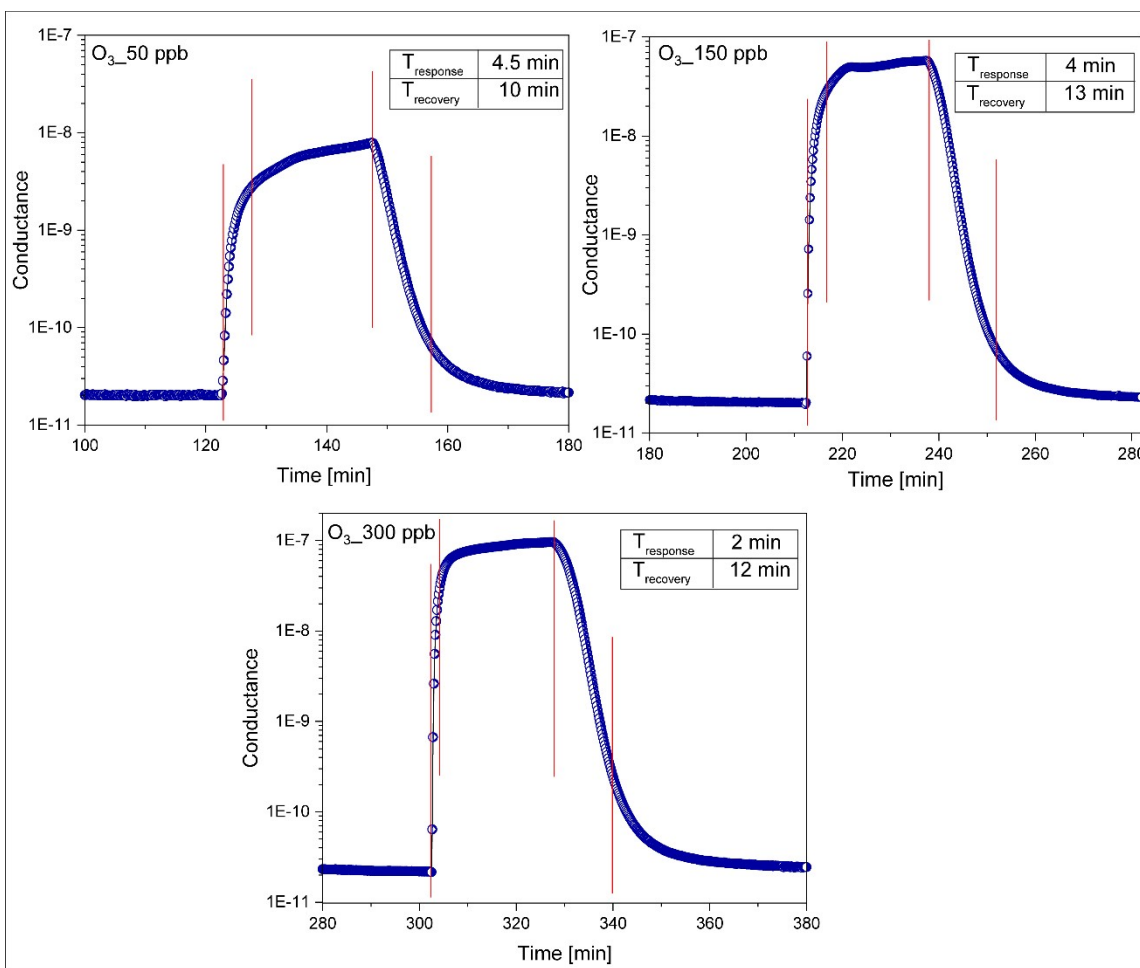


Figure S1. Response and recovery time of NWO heterostructure sensors towards ozone (50_150_300 ppb) at 300 °C, Inserted tables report the calculated values of response and recovery time for each gas concentration.

Stability measurement

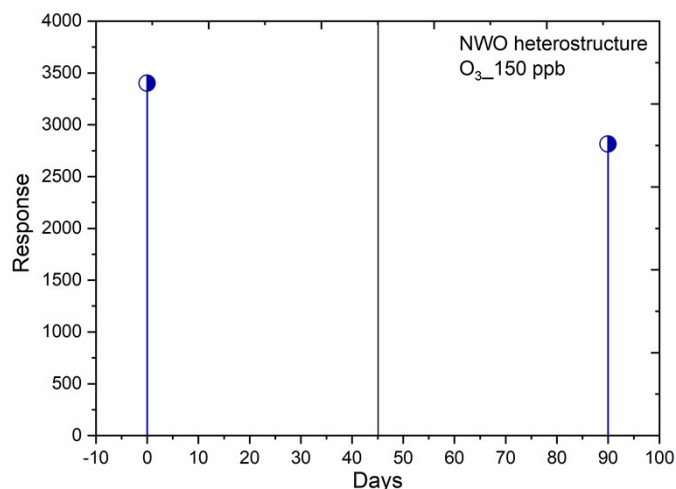


Figure S2. Response comparison of NWO heterostructure sensors towards ozone _150 ppb at 300 °C on the first day and after 3 months.

Detection Limits of Sensor

In order to determine the detection limits toward ozone molecules, the calibration curves (graph response vs O₃ different concentrations) at 300 °C and 400 °C for pristine NiO and NWO heterostructure sensors for ozone were determined and are shown in Figure 3d (manuscript). It can be seen from Figure 3d that the slope of calibration curves for NWO sensors is different from the pristine NiO NWs. This is the indication of a different reaction mechanism of both sensors when reacting with ozone molecules. This is due to the presence of WO₃ and NiWO₄ in their interaction with ozone. Furthermore, the estimation of the detection limits was done by fitting the experimental data of calibration curves by following a power trend law for metal oxides,

$$\text{Response} = A [\text{gas concentration}]^B$$

Here A and B are typically related to the sensing material and the stoichiometry involved in the chemical reaction. By considering the response value = 1 (as a minimum response to get a detectable signal), the detection limits for the sensors were determined at 300 and 400 °C and are presented in Table S1. The NWO sensors show the lowest detection limit of 0.2 ppb at 300 °C.

Table S1. Detection limits of NWO and NiO sensors.

| Sensor | A | B | Detection limits |
|--------------|-----|-----|------------------|
| NWO (300 °C) | 6.8 | 1.2 | 0.2 ppb |
| NiO (300 °C) | 1.2 | 1.1 | 0.8 ppb |
| NWO (400 °C) | 1.6 | 0.8 | 0.6 ppb |
| NiO (300 °C) | 0.3 | 0.9 | 3.6 ppb |

Literature Comparison

The sensing performance of both fabricated pristine NiO nanowires (NWs) and the NiWO₄ (NWO) 3D nano-heterostructures was compared with various reports published in the literature. This comparison is presented in Table S2 below, where different physical parameters such as concentration, sensor operating temperature, and response value were considered.

Directly comparing our fabricated sensors with existing data poses challenges, as no similar type of heterostructure has been previously tested for ozone detection. However, the data presented in the table S2 indicates that the NWO heterostructure exhibited superior sensing performance compared to both bare and modified NiO and WO₃ nanostructures, as well as other heterostructures and 2D materials.

Table S2. Comparison of NWO and NiO nanowires sensor performance with literature.

| Material | Strategies | Ozone concentration | Working temperature | Response | ref |
|-------------------------------|------------|---------------------|---------------------|----------|--------------|
| WO ₃ | Thin film | 800 ppb | 250 °C | 310 | ¹ |
| WO ₃ | Thin film | 800 ppb | 300 °C | 7.6 | ² |
| Au- WO ₃ | Thin film | 800 ppb | 300 °C | 78 | ² |
| Co/WO ₃ | Thin film | 0.8 ppm | 250 °C | 3.5 | ³ |
| Al-NiO | Thin film | 207 ppb | 150 °C | 1.39 | ⁴ |
| V ₂ O ₅ | Nanowires | 1 ppm | 300 °C | 0.1 | ⁵ |

| | | | | | |
|-------------------|------------------|--------------------|--------|--------------|-----------|
| V_2O_5/TiO_2 | Heterostructures | 1 ppm | 300 °C | 1.4 | 5 |
| $CuWO_4$ | Nanoparticles | 90 ppb | 250 °C | 10 | 6 |
| In_2O_3/ZnO | Heterostructures | 50 ppb | 110 °C | 6.7 | 7 |
| $Zn:MoS_2$ | Nanosheets | 5000 ppb | RT | 0.9 | 8 |
| $Bi_2Fe_4O_9$ | Nanosheets | 100,000 ppb | 260 °C | 7.5 | 9 |
| WO_3 | Nanowires | 300 ppb | 200 °C | 170 | 10 |
| NiO | Nanowires | 300 ppb | 300 °C | 567 | This work |
| $NiO/NiWO_4/WO_3$ | Heterostructures | 150 ppb 300 ppb | 300 °C | 3107 4704 | This work |

References

- 1 M. Bendahan, R. Boulmani, J. L. Seguin and K. Aguir, *Sensors Actuators, B Chem.*, , DOI:10.1016/j.snb.2004.01.023.
- 2 A. Labidi, E. Gillet, R. Delamare, M. Maaref and K. Aguir, *Sensors Actuators, B Chem.*, 2006.
- 3 W. Belkacem, A. Labidi, J. Guérin, N. Mliki and K. Aguir, *Sensors Actuators, B Chem.*, , DOI:10.1016/j.snb.2008.01.023.
- 4 A. Paralikis, E. Gagaoudakis, V. Kampitakis, E. Aperathitis, G. Kiriakidis and V. Binas, *Appl. Sci.*, , DOI:10.3390/app11073104.
- 5 W. Avansi, A. C. Catto, L. F. Da Silva, T. Fiorido, S. Bernardini, V. R. Mastelaro, K. Aguir and R. Arenal, *ACS Appl. Nano Mater.*, , DOI:10.1021/acsanm.9b00578.
- 6 A. C. Catto, T. Fiorido, É. L. S. Souza, W. Avansi, J. Andres, K. Aguir, E. Longo, L. S. Cavalcante and L. F. da Silva, *J. Alloys Compd.*, , DOI:10.1016/j.jallcom.2018.03.104.
- 7 N. Sui, Y. Xu, P. Zhang, S. Cao, T. Zhou and T. Zhang, *Sensors Actuators B Chem.*, , DOI:10.1016/j.snb.2023.133312.

- 8 L. Shao, Z. Wu, H. Duan and T. Shaymurat, *Sensors Actuators, B Chem.*, , DOI:10.1016/j.snb.2017.11.166.
- 9 J. Yang, J. Gao, P. Fu, Z. Chen, S. Wang, L. Liu and Z. Lin, *Mater. Res. Express*, , DOI:10.1088/2053-1591/ab31b3.
- 10 N. Kaur, D. Zappa, N. Poli and E. Comini, *ACS Omega*, , DOI:10.1021/acsomega.9b01792.